

Supporting Information

Zinc Ions and Zinc-Embedded Carbon Quantum Dots as Competitive Inhibitors of Fumarase: Preferential Inhibition of the Reverse Reaction

Amene Navaser^a, Hamid R. Kalhor^{*a,b}

Address: ^aBiochemistry and Chemical Biology Research Laboratory, Chemistry Department, Sharif University of Technology, Tehran, Iran.

^bInstitute for Convergence Science & Technology, Sharif University of Technology, Tehran, Iran.

Email: *Hamid Reza Kalhor - kalhor@sharif.edu Tel: +982166165315 Fax: +982166165315

Contents

Experimental section	4
Material and methods	4
General procedure for infrared (IR) spectra	4
General procedure for photoluminescence (PL) spectroscopy	4
General procedure for UV-Visible spectroscopy	4
General procedure for X-ray diffraction (XRD) analysis	4
General Procedure for circular dichroism (CD) spectrophotometry	5
General Procedure for SDS-page acrylamide gel electrophoresis	5
Experimental.....	5
The expression of recombinant fumarate hydratase	5
Purification of Fumarase Using Ni-NTA Affinity Chromatography	6
Fumarate hydratase activity assay	6
Enzyme concentration determination	7
Fumarate hydratase activity assay in the presence of metal salts	7
The kinetics study of fumarate hydratase	7
Statistical Analysis of Enzyme Kinetic	8
Calculating 95% Confidence Intervals (CI)	8
Optimizing Zn(1)-CQDs concentration for fumarase inhibitory	9
Synthesizing Zn(0.5)-CQDs	9
Synthesizing Zn(1)-CQDs	9
Synthesizing Zn(2)-CQDs	9
Synthesizing N-doped CQDs	10
Zn(1)-CQD solubility	10
Quantitative Analysis of Acid/Base Sites on Zn-CQDs	10
Antibacterial Assay of Fumarase Inhibition Complexes	11
Fumarase Activity Assay Using Cell Free Extracts	11
Molecular Docking	12
Molecular Docking Method Validation	12
Molecular Dynamics (MD) Simulations	12
Tables.....	14
Table S1. Fumarate to L-malate Kinetics with Statistical Analysis (pairs t-test)	14
Table S2. L-malate to Fumarate Kinetics with Statistical Analysis (pairs t-test)	14

Table S3. Mean \pm SD and 95% Confidence Intervals for Kinetic Parameters of Fumarase	15
Figures	16
Figure S1.	16
Figure S2.	16
Figure S3.	17
Figure S4.	17
Figure S5.	18
Figure S6.	18
Figure S7.	18
Figure S8	19
Figure S9.	19
Figure S10.	20
References	20

Experimental section

Material and methods

All chemical reagents and materials were purchased from Sigma-Aldrich® and used as received, without further purification. Infrared (IR) spectra were recorded using a Perkin Elmer Spectrum Two IR spectrometer. UV-Visible absorption spectra were measured using an Agilent Cary 100 Bio Varian spectrophotometer. Photoluminescence properties of the carbon quantum dots (CQDs) were analyzed using a Cary Eclipse Varian fluorescence spectrometer. Scanning electron microscopy (SEM) images were obtained using a Mira 3 scanning electron microscope. Circular dichroism (CD) measurements were performed on a JASCO model J-715 CD spectrometer at 25 °C. X-ray diffraction (XRD) patterns of zinc modified CQDS (Zn-CQD) were collected in the 2θ range of 10° to 80° using a PANalytical XPert PRO MPD diffractometer.

General procedure for infrared (IR) spectra

The infrared (IR) spectra were recorded on a Perkin Elmer Spectrum Two IR spectrometer. The sample was prepared by mixing the analyte with potassium bromide (KBr) and pressing the mixture into a pellet. Spectra were acquired in the range of $4000\text{--}500\text{ cm}^{-1}$, with KBr as the background reference.

General procedure for photoluminescence (PL) spectroscopy

A solution containing 1 mg of nanoparticles dissolved in 5 mL of deionized water was prepared. The photoluminescence properties of the solution were investigated using a VARIAN Cary Eclipse fluorescence spectrophotometer, with excitation wavelengths ranging from 240 nm to 440 nm.

General procedure for UV-Visible spectroscopy

A solution of 0.2 mg of nanoparticles dissolved in 2 mL of deionized water was prepared. UV-Visible absorption spectra were recorded using an Agilent Cary 100 Bio Varian spectrophotometer in the range of 200 to 600 nm.

General procedure for X-ray diffraction (XRD) analysis

The XRD pattern of Zn-CQD was recorded in the 2θ range of 10° to 80° using a PANalytical XPert PRO MPD diffractometer.

General Procedure for circular dichroism (CD) spectrophotometry

Three samples were prepared as follows:

Free enzyme sample: 200 μ M fumarase in 50 mM phosphate buffer pH 7.

ZnCl₂ sample: 200 μ M fumarase, 200 μ M ZnCl₂ in 50 mM phosphate buffer pH 7.

Zn(1)-CQDs sample: 200 μ M fumarase, 150 μ g/mL Zn-CQDs in 50 mM phosphate buffer pH 7.

Circular dichroism (CD) measurements were conducted following the addition of the inhibitor to enzyme using a JASCO model J-715 CD spectrometer at 25 °C. The data are presented as molar ellipticity, $[\theta] \times 10^{-3}$ (deg·cm²/dmol).

General Procedure for SDS-page acrylamide gel electrophoresis

The 16% acrylamide resolving gel solution was prepared by combining 3.833 mL of deionized water, 3.52 mL of 30% acrylamide-bisacrylamide solution, 2.5 mL of Tris-HCl buffer (1.5 M, pH 8.8), 100 μ L of 10% (w/v) SDS, 50 μ L of 10% (w/v) ammonium persulfate (APS), and 25 μ L of tetramethylethylenediamine (TEMED).

The 4% acrylamide stacking gel solution was prepared by mixing 3 mL of deionized water, 0.62 mL of 30% acrylamide-bisacrylamide solution, 1.26 mL of Tris-HCl buffer (0.5 M, pH 6.8), 50 μ L of 10% (w/v) SDS, 25 μ L of 10% (w/v) APS, and 30 μ L of TEMED.

Electrophoresis was performed at 45 V for the stacking gel and 75 V for the resolving gel. The acrylamide gel was stained using Coomassie Brilliant Blue R-250 solution. For sample preparation, 10 μ L of 5 \times Laemmli buffer was thoroughly mixed with 40 μ L of each sample.

Experimental

The expression of recombinant fumarate hydratase

A single colony of pre-cultured *E. coli* BL21 (DE3) harboring the pET-26b-(+)/fumarase (*saccharomyces cerevisiae* fumarate hydratase) plasmid was inoculated into 5 mL of Lysogeny Broth (LB) medium supplemented with kanamycin at a final concentration of 100 μ g/mL. The culture was incubated overnight at 37 °C with shaking at 180 rpm. The overnight culture was then used to

inoculate 500 mL of LB medium in a 1 L flask, supplemented with kanamycin at a final concentration of 100 $\mu\text{g}/\text{mL}$, to an initial optical density (OD_{600}) of 0.025. The culture was incubated at 37 °C with shaking at 180 rpm until the OD_{600} reached 0.6-0.8. Protein expression was induced by the addition of IPTG to a final concentration of 0.4 mM, and the culture was incubated overnight at 15 °C with shaking.

The cells were harvested by centrifugation at 4,000 rpm for 20 minutes at 4 °C and were resuspended in 50 mL of lysis buffer (50 mM NaH_2PO_4 pH 8.5, 300 mM NaCl, 1 mM PMSF) and subjected to sonication for 20 minutes (6 seconds on, 4 seconds off) on ice. The lysate was clarified by centrifugation at 12,000 rpm for 10 minutes at 4 °C to remove cellular debris. The supernatant containing the soluble proteins was carefully collected for further purification

Purification of Fumarase Using Ni-NTA Affinity Chromatography

The protein solution was applied to a pre-equilibrated Ni-NTA resin column (HisPur™, Thermo Fisher Scientific), which had been equilibrated with 50 mM NaH_2PO_4 , 500 mM NaCl, pH 8.0. The flow-through was collected, and the column was washed with two successive buffers to remove unbound proteins:

wash 1: 50 mM NaH_2PO_4 , 500 mM NaCl, and 50 mM imidazole, pH 8.5.

wash 2: 50 mM NaH_2PO_4 , 500 mM NaCl, and 80 mM imidazole, pH 8.5.

Following the washes, the protein was eluted with a 400 mM imidazole solution in 50 mM NaH_2PO_4 , 500 mM NaCl, pH 8.5. Fractions were collected and analyzed for the presence of fumarase by SDS-PAGE (Figure S1). The fractions containing the purified fumarase were pooled and dialyzed against 20 mM NaCl solution for 6 hours at 0 °C to remove excess imidazole. The final protein solution was concentrated using a stirred ultrafiltration cell (Amicon®, 2 kD cutoff filter) to the desired concentration and either used immediately for further experiments or stored at -80 °C.

Fumarate hydratase activity assay

Fumarate hydratase activity was measured by monitoring the increase in absorbance at 250 nm, which corresponds to the conversion of L-malate to fumarate. A 2 mL reaction mixture containing 50 mM phosphate buffer (pH 7.0) and 20 μM fumarate hydratase was prepared. The reaction was initiated by the addition of 5 mM L-malic

acid. The reaction proceeded at 30 °C for 10 minutes. The increase in absorbance at 250 nm, corresponding to the conversion of L-malate to fumarate, was monitored over time. The rate of absorbance increase confirmed the fumarate hydratase activity (Figure S2).

A blank reaction was prepared containing 50 mM phosphate buffer (pH 7.0) and 20 μ M fumarate hydratase ensuring that the observed increase in absorbance was solely attributed to the conversion of L-malate to fumarate.

A control reaction was performed without enzyme to account for any background absorbance changes. The fumarate hydratase activity was calculated by subtracting the non-enzymatic background from the total absorbance change.

Enzyme concentration determination

The absorbance of the purified fumarate hydratase enzyme solution was measured at 280 nm, then the enzyme concentration was determined using the concentration of the enzyme was calculated using Beer-Lambert's law and theoretical extinction coefficient 280 nm of 24410 $M^{-1} cm^{-1}$.

Fumarate hydratase activity assay in the presence of metal salts

Fumarate hydratase activity in the presence of metal salt was measured by monitoring the increase in absorbance at 250 nm, which corresponds to the conversion of L-malate to fumarate. A 2 mL reaction mixture containing 50 mM phosphate buffer (pH 7.0), 200 μ M metal salts, and 20 μ g. mL^{-1} fumarate hydratase was prepared. The reaction was initiated by the addition of substrate (L-malic acid or fumarate). The reaction proceeded at 30 °C for 10 minutes. The increase or decrease in absorbance at 250 nm, corresponding to the conversion was monitored over time.

The kinetics study of fumarate hydratase

To determine the enzyme kinetics, the assay was performed with varying concentrations of L-malic acid (0.4 mM to 1 mM) or fumaric acid (0.1 mM to 4 mM). The initial velocity of the reaction was determined for each substrate concentration by measuring the change in absorbance at 250 nm over 60 seconds. A 2 mL reaction mixture containing 50 mM phosphate buffer (pH 7.0) and 10 μ M fumarate hydratase was prepared. For the inhibition kinetics, 200 μ M of the $ZnCl_2$ or 150 μ g/mL of Zn-CQD were added to the reaction mixture, and the reaction was initiated by the addition of L-malate or fumarate. The reaction was initiated by the

addition of L-malic acid or fumaric acid. The reciprocal of the initial velocity ($1/v_0$) was plotted against the reciprocal of the substrate concentration ($1/[S]$) to generate a Lineweaver-Burk plot. Kinetic parameters, including the Michaelis constant (K_m) and maximum velocity (V_{max}), were derived from the following Lineweaver-Burk equation:

$$\frac{1}{v_0} = \frac{K_m}{V_{max}} \cdot \frac{1}{[S]} + \frac{1}{V_{max}}$$

The inhibition constant was derived from the following equation:

$$K_i = \frac{[I]}{\frac{K_m \text{ in the presence of inhibitor}}{K_m \text{ in the absence of inhibitor}} - 1}$$

Where the K_i is the Inhibition constant, K_m is the Michaelis constant of the enzyme, and [I] is the inhibitor concentration.

V_{max} was obtained from the Lineweaver–Burk plot and subsequently normalized to the enzyme mass (mg protein) used in the assay, giving final units of $\mu\text{mol}\cdot\text{min}^{-1}\cdot\text{mg}^{-1}$.

Each experiment repeated three times and the average absorbance was used for plotting.

Statistical Analysis of Enzyme Kinetic

Each kinetic experiment (fumarate to L-malate and L-malate to fumarate) was performed in triplicate using independently prepared enzyme samples. To assess statistical significance of differences between experimental groups (free enzyme, Zn^{2+} -treated, and Zn(1)-CQDs-treated) pairwise comparisons were conducted using two sample assuming unequal variances t-tests (Tables S1 and S2).

Calculating 95% Confidence Intervals (CI)

To quantify the precision of the kinetic parameters K_m and V_{max} For each group (Free Enzyme, Zn^{2+} -treated, and Zn(1)-CQDs-treated), the following equations were used and the results are presented in Table S3:

$$\text{Lower CI} = \text{Mean} - t_{crit} \times SE$$

$$\text{Upper CI} = \text{Mean} + t_{crit} \times SE$$

Where the t_{crit} is the t critical value, Mean is the average of the three replicant for each parameter, and the SE represents standard error.

Optimizing Zn(1)-CQDs concentration for fumarase inhibitory

To determine the optimum Zn(1)-CQDs concentration, the assay was performed with varying concentrations of L-malic acid (0.4 mM to 1 mM) or fumaric acid (0.1 mM to 4 mM). The initial velocity of the reaction was determined for each substrate concentration by measuring the change in absorbance at 250 nm over 60 seconds. A 2 mL reaction mixture containing 50 mM phosphate buffer (pH 7.0) and 10 μ M fumarate hydratase, different concentration of Zn(1)-CQDs (50, 100, and 150 μ g/mL) was prepared and the reaction initiated by adding L-malic acid or fumaric acid. The corresponding Lineweaver-Burk plots are shown in Figure S3.

Synthesizing Zn(0.5)-CQDs

A 1:1:0.5 stoichiometric ratio of citric acid:urea:ZnCl₂ was used to synthesize Zn(0.5)-CQD. Specifically, 10 mmol of citric acid (1.92 g), 10 mmol of urea (0.6 g), and 5 mmol of ZnCl₂ (0.68 g) were dissolved in 50 mL of distilled water. The mixture was stirred until a colorless, uniform solution was obtained. This solution was then transferred to a vacuum oven and heated at 150°C for 3 hours, resulting in the formation of a brown solid. The brown solid was dissolved in distilled water and dialyzed using a 2 kDa dialysis bag for 6 hours against distilled water. Finally, the dialyzed solution was dried, yielding the Zn(0.5)-CQDs product.

Synthesizing Zn(1)-CQDs

A 1:1:1 stoichiometric ratio of citric acid:urea:ZnCl₂ was used to synthesize Zn(1)-CQD. Specifically, 10 mmol of citric acid (1.92 g), 10 mmol of urea (0.6 g), and 10 mmol of ZnCl₂ (1.36 g) were dissolved in 50 mL of distilled water. The mixture was stirred until a colorless, uniform solution was obtained. This solution was then transferred to a vacuum oven and heated at 150°C for 3 hours, resulting in the formation of a dark brown solid. The brown solid was dissolved in distilled water and dialyzed using a 2 kDa dialysis bag for 6 hours against distilled water. Finally, the dialyzed solution was dried, yielding the Zn(1)-CQDs product.

Synthesizing Zn(2)-CQDs

A 1:1:2 stoichiometric ratio of citric acid:urea:ZnCl₂ was used to synthesize Zn(2)-CQD. Specifically, 10 mmol of citric acid (1.92 g), 10 mmol of urea (0.6 g), and 20

mmol of ZnCl_2 (2.72 g) were dissolved in 50 mL of distilled water. The mixture was stirred until a colorless, uniform solution was obtained. This solution was then transferred to a vacuum oven and heated at 150°C for 3 hours, resulting in the formation of a brown aggregated solid. The brown solid was dissolved in distilled water and dialyzed using a 2 kDa dialysis bag for 6 hours against distilled water. Finally, the dialyzed solution was dried, yielding the Zn(2)-CQDs product.

Synthesizing N-doped CQDs

A 1:1 stoichiometric ratio of citric acid:urea was used to synthesize N-doped CQD. Specifically, 10 mmol of citric acid (1.92 g) and 10 mmol of urea (0.6 g) were dissolved in 50 mL of distilled water. The mixture was stirred until a colorless, uniform solution was obtained. This solution was then transferred to a vacuum oven and heated at 150°C for 3 hours, resulting in the formation of a black solid. The black solid was dissolved in distilled water and dialyzed using a 2 kDa dialysis bag for 6 hours against distilled water. Finally, the dialyzed solution was dried, yielding the N-doped CQDs product.

Zn(1)-CQD solubility

A precise mass (500 mg) of Zn-CQDs was weighed and dispersed in 2 mL deionized water in a glass vial. The dispersion was sonicated for 30 min to achieve maximum solubility followed by continuous stirring at room temperature for 12 h. The dispersion was allowed to settle for 30 min before being passed through a $0.22\ \mu\text{m}$ syringe filter to remove any undissolved particles. To further clarify, the filtrate was centrifuged at 14000 rpm for 15 min. The supernatant was transferred to a pre-weighed glass vial and dried until a constant mass was achieved. The solubility as determined 180 mg/mL.

Quantitative Analysis of Acid/Base Sites on Zn-CQDs

Quantitative analysis of the acid/base sites of Zn-CQDs was performed following a titration-based method. Typically, 4.5 mg of Zn-CQDs was dispersed in 1 mL of deionized water, and the solution was mixed with 1 mL of 0.5 M NaOH. The resulting mixture was titrated with 0.1 M HCl. Each titration was performed in triplicate. A Gran plot was used to determine the total acid/base sites. After calculating the values of $\mu\text{mol}_{\text{eq}1}$ and $\mu\text{mol}_{\text{eq}2}$, the total number of acid/base sites was obtained by subtracting $\mu\text{mol}_{\text{eq}2}$ from $\mu\text{mol}_{\text{eq}1}$ and normalizing the result to the amount of Zn-CQDs used.

Antibacterial Assay of Fumarase Inhibition Complexes

Escherichia coli BL21 (DE3) was used as the model strain. Cells were cultured in LB medium at 37 °C with shaking at 200 rpm. For the assay, overnight cultures were diluted 1:100 in fresh LB medium. Three experimental groups were prepared: untreated cells (no inhibitors), cell treated with ZnCl₂ (5 mg in 20 mL LB medium) and, cell treated with Zn(1)-CQDs (5 mg in 20 mL LB medium). fumarate was added at increasing concentrations (0, 1, 5, 10, and 15 mM) to each treatment group. OD₆₀₀ values were recorded every 60 minutes over 5 hours using a UV-Vis spectrophotometer. Growth curves were plotted (Figure S5). All experiments were performed in triplicate.

Fumarase Activity Assay Using Cell Free Extracts

E.coli BL21 cells expressing recombinant fumarase were grown under three conditions: untreated (control), treated with ZnCl₂ (1 mg/mL), and treated with Zn(1)-CQDs (1 mg/mL). Cells were harvested by centrifugation at 4000 × g for 10 min. Cell pellets were resuspended in 50 mM phosphate buffer (pH 7) and lysed by sonication on ice for 30 min. The lysates were clarified by centrifugation at 12,000 × g for 15 min, and the supernatant was used for enzymatic assays. Total protein concentration in the lysates was determined using the Bradford assay with BSA as the standard¹. Fumarase activity was assessed in both the forward and reverse directions: 1) In the forward reaction (L-malate to fumarate), activity was monitored by measuring the increase in absorbance at 250 nm due to the formation of fumarate, 2) In the reverse reaction (fumarate to L-malate), the decrease in absorbance at 250 nm was followed, indicating the consumption of fumarate. Each assay was carried out in 2 mL phosphate buffer (50 mM, pH 7) at 25 °C. The substrate (either sodium L-malate or fumarate) was used at a final concentration of 5 mM, and the reaction was initiated by adding 50 µg/mL of total protein from the clarified cell lysate. Absorbance at 250 nm was recorded every minute for 10 minutes using a UV-visible spectrophotometer. Blank samples lacking substrate were used for baseline correction.

Each experiment repeated three times and the average absorbance was used for plotting.

Molecular Docking

To investigate the interaction of Zn^{2+} with fumarase, molecular docking simulations were performed using AutoDock Vina. The crystal structure of *Saccharomyces cerevisiae* fumarase (PDB ID: 1YFM) was retrieved from the Protein Data Bank (PDB) and prepared using AutoDockTools by adding hydrogen atoms and removing water molecules. The Zn^{2+} ion was modeled using Avogadro², saved in PDB format, and subsequently converted to PDBQT format using AutoDockTools³ for docking compatibility.

Docking was carried out with a grid box encompassing the entire tetrameric structure to allow for an unbiased search of potential Zn^{2+} binding sites. An exhaustiveness value of 256 was used to ensure thorough conformational sampling. The default AutoDock Vina scoring function was applied to rank binding poses, and the top-ranked pose was selected for further analysis. Other binding poses were illustrated in Figure S6.

Molecular Docking Method Validation

To validate the docking methodology, we performed a control docking experiment using streptococcal pyrogenic exotoxin A (SpeA), a known Zn^{2+} -binding superantigen, using its zinc-bound crystal structure (PDB ID: 1HA5)⁴. The native Zn^{2+} ions were removed from the crystal structure to generate an apo-protein model. Then, one Zn^{2+} was then re-docked to the apo-protein using the same docking protocol as for fumarase. The results demonstrated that Zn^{2+} re-docked almost the original binding site, validating the reliability of our docking parameters and methodology (Figure S7).

Molecular Dynamics (MD) Simulations

Molecular dynamics (MD) simulations were conducted using GROMACS 2020⁵ with the CHARMM27 force field to investigate the structural dynamics of fumarase in the presence and absence of Zn^{2+} ions. The same simulation protocol was applied to both systems. The initial structures were obtained from molecular docking studies (top-ranked pose). The simulation system was solvated in a Simple Point Charge (SPC) water model within a cubic simulation box, ensuring a minimum distance of 1.0 nm between the protein and the box edges. Counterions were added to neutralize

the system. Energy minimization was performed using the steepest descent algorithm until the maximum force was below $1000 \text{ kJ mol}^{-1} \text{ nm}^{-1}$. Equilibration was carried out in two phases: (i) NVT ensemble at 300 K for 100 ps, followed by (ii) NPT ensemble for 100 ps to stabilize the system. The V-rescale thermostat and Parrinello-Rahman barostat were applied to maintain temperature and pressure, respectively. The production run was conducted for 10 ns using a 2 fs time step.

Tables

Table S1. Fumarate to L-malate Kinetics with Statistical Analysis (pairs t-test).

Comparison	Parameter	Group 1	Group 2	Mean (Group 1)	Mean (Group 2)	t Stat	p-value (two-tailed)
Free enzyme (FE) vs Zn ²⁺	K_m	FE	Zn ²⁺	1.10	6.72	-57.20	0.000005
	K_{cat}	FE	Zn ²⁺	617.02	637.51	-2.57	0.1237
	V_{max}	FE	Zn ²⁺	347.81	351.60	-2.57	0.1237
Free enzyme (FE) vs Zn-CQD	K_m	FE	Zn(1)-CQD	1.10	8.12	-17.66	0.003
	K_{cat}	FE	Zn(1)-CQD	617.02	610.74	-0.57	0.6074
	V_{max}	FE	Zn(1)-CQD	347.81	347.54	-0.57	0.6074
Zn-CQD vs Zn ²⁺	K_m	Zn ²⁺	Zn(1)-CQD	6.72	8.12	-4.34	0.0491
	K_{cat}	Zn ²⁺	Zn(1)-CQD	637.51	610.74	2.80	0.677
	V_{max}	Zn ²⁺	Zn(1)-CQD	351.60	347.54	2.80	0.677
	K_i	Zn ²⁺	Zn(1)-CQD	39.14	23.50	3.83	0.0185

Table S2. L-malate to Fumarate Kinetics with Statistical Analysis (pairs t-test).

Comparison	Parameter	Group 1	Group 2	Mean (Group 1)	Mean (Group 2)	t Stat	p-value (two-tailed)
Free enzyme (FE) vs Zn ²⁺	K_m	FE	Zn ²⁺	1.58	131.95	-96.68	0.0001
	K_{cat}	FE	Zn ²⁺	595.74	591.82	1.19	0.3558
	V_{max}	FE	Zn ²⁺	338.09	334.55	0.58	0.6152
Free enzyme (FE) vs Zn-CQD	K_m	FE	Zn(1)-CQD	1.58	221.32	-67.65	0.0002
	K_{cat}	FE	Zn(1)-CQD	595.74	596.07	0.9763	0.4318
	V_{max}	FE	Zn(1)-CQD	338.09	336.18	0.4829	0.6768
Zn-CQD vs Zn ²⁺	K_m	Zn ²⁺	Zn(1)-CQD	131.95	221.32	-25.68	0.0001
	K_{cat}	Zn ²⁺	Zn(1)-CQD	591.82	596.07	-0.7913	0.4730
	V_{max}	Zn ²⁺	Zn(1)-CQD	334.55	336.18	-0.7913	0.4730
	K_i	Zn ²⁺	Zn-CQD	2.42	1.08	4.22	0.0243

Table S3. Mean \pm SD and 95% Confidence Intervals for Kinetic Parameters of Fumarase.

Reaction Direction	Group	Mean \pm SD	K_m (mM)		Mean \pm SD	V_{max} (μ mol/min/mg)	
			Lower CI	Upper CI		Lower CI	Upper CI
Forward Reaction	Free Enzyme	1.10 \pm 0.12	0.78	1.41	347.81 \pm 1.96	342.92	352.69
	Zn ²⁺	6.72 \pm 0.12	6.41	7.02	351.60 \pm 3.0	344.13	359.06
	Zn(1)-CQD	8.12 \pm 0.24	7.52	9.97	347.54 \pm 7.43	329.07	366.01
Reverse Reaction	Free Enzyme	1.58 \pm 0.32	0.7645	2.39	338.09 \pm 7.46	319.55	356.62
	Zn ²⁺	131.95 \pm 2.35	126.09	137.81	334.55 \pm 7.39	316.18	352.91
	Zn(1)-CQD	221.32 \pm 5.75	207.01	235.61	336.18 \pm 6.92	318.96	353.39

Figures

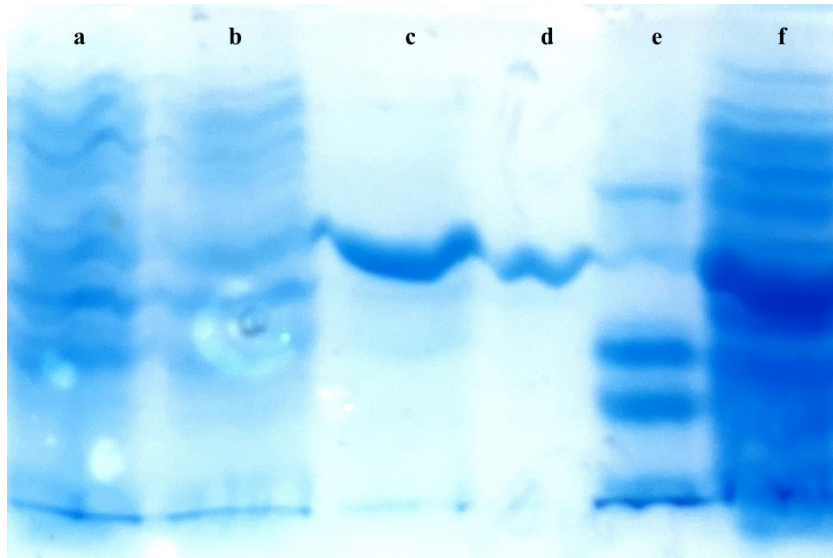


Figure S1. SDS-PAGE of protein purification. Lane (a) first wash, (b) second wash, (c) eluted protein fraction, (d) purified protein after dialysis, (e) protein marker, and (f) supernatant following cell lysis. The gel demonstrates the purification progress, with the protein band sizes corresponding to molecular weight standards indicated by the

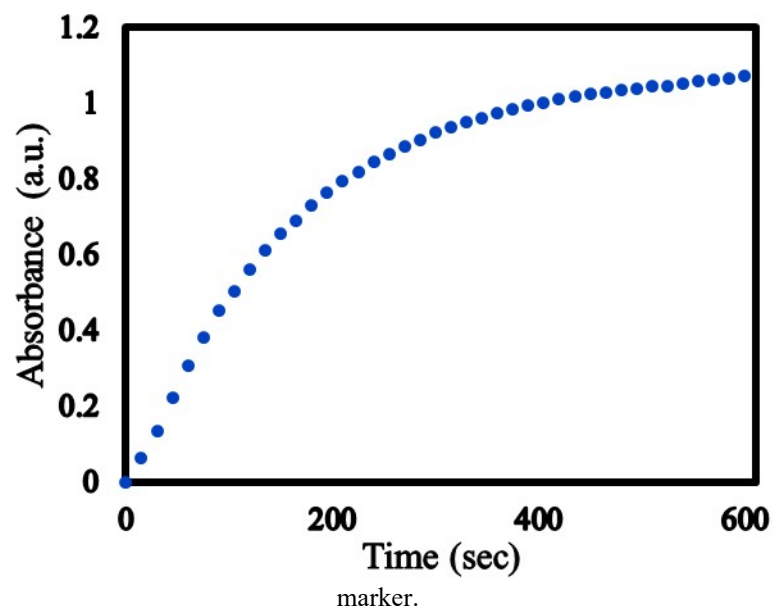


Figure S2. Fumarate hydratase activity assay. The reaction was carried out in a 2 mL mixture containing 50 mM phosphate buffer pH 7, 20 μ M fumarate hydratase, and 30 mM L-malate at 30°C for 10 minutes. The plot shows the time-dependent increase in absorbance, reflecting the enzymatic conversion of L-malate to fumarate.

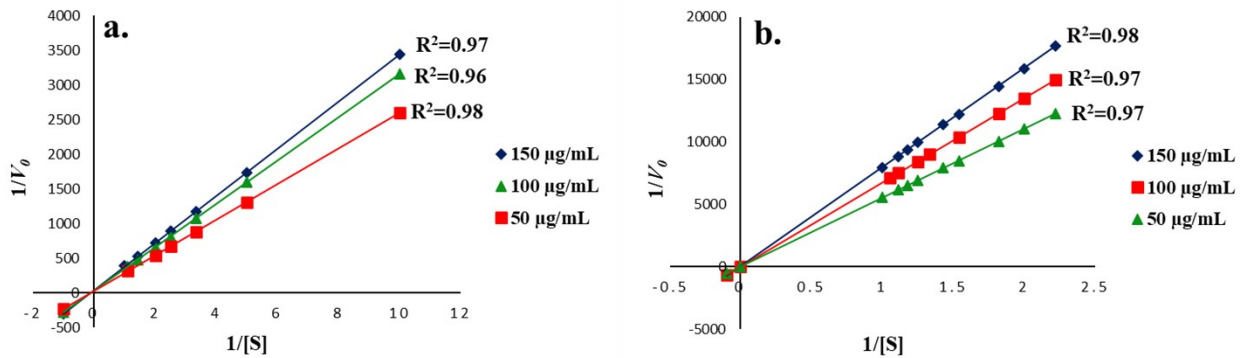


Figure S3. Lineweaver-Burk plots for determining the optimum concentration of Zn(1)-CQDs. The initial velocities of the fumarate hydratase reaction were measured at varying concentrations of (a) L-malic acid (0.4 mM to 1 mM) or (b) fumaric acid (0.1 mM to 4 mM) in the presence of 50 µg/mL Zn(1)-CQDs (green line), 100 µg/mL Zn(1)-CQDs (red line), and 150 µg/mL Zn(1)-CQDs (blue line). Each time point is an average of three independent experiments.

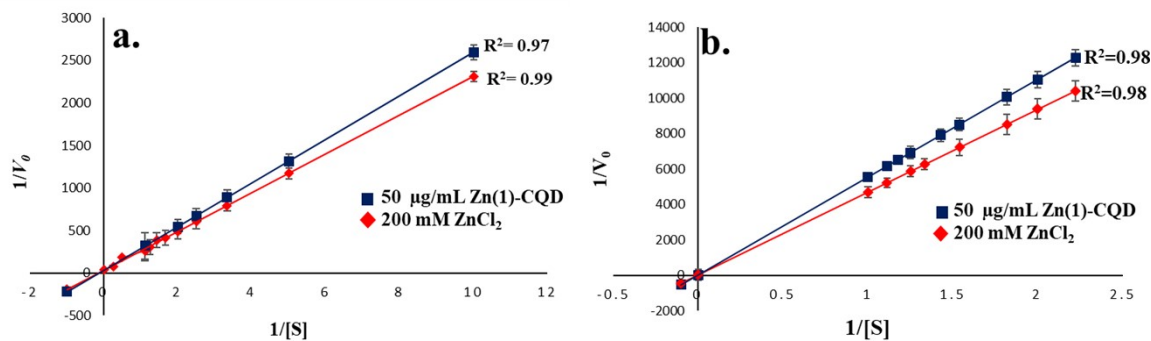


Figure S4. Lineweaver-Burk plots in the presence of (a) ZnCl₂ (200 µM; ≈0.20 µmol Zn²⁺) and (b) Zn(1)-CQDs (50 µg/mL; ≈0.16 µmol Zn²⁺). The plots demonstrate that Zn-CQDs exert slightly stronger inhibitory effects than free Zn²⁺ at comparable Zn concentrations.

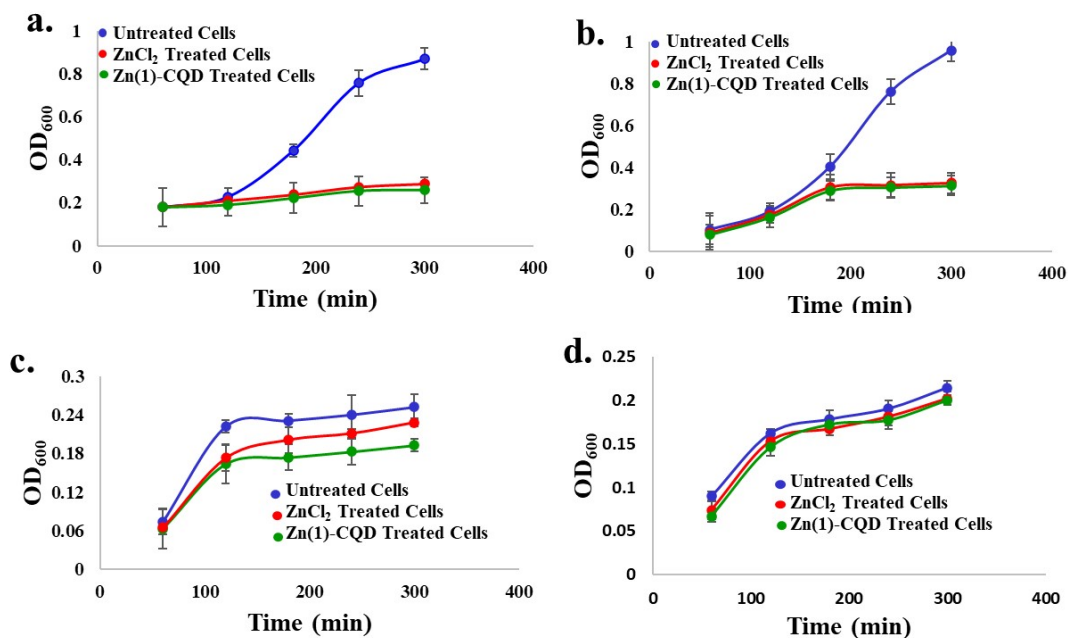


Figure S5. Growth curves of *E. coli* BL21 cells without treatment (blue), Zn^{2+} ions treated cells (red), and Zn(1)-CQD treated cells (green) in the presence of (a) 0 mM fumarate, (b) 1mM fumarate, (c) 5 mM fumarate, and (d) 15 mM fumarate.

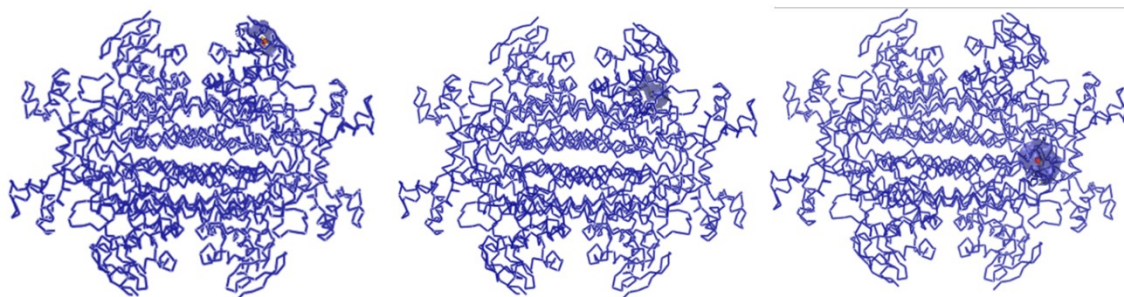
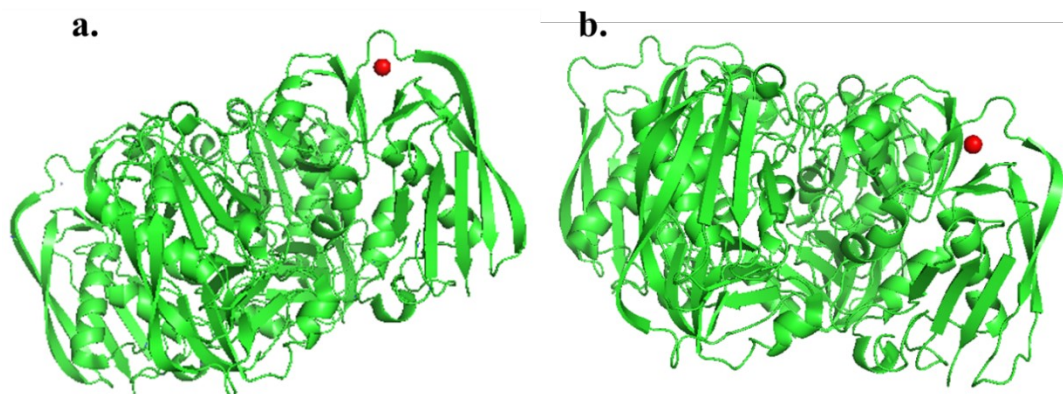


Figure S6. Zn^{2+} docked into the fumarase structure, other binding poses of Zn^{2+} . Zn^{2+} represented as red bead and



the binding site is represented as transparent surface.

Figure S7. The validity of molecular docking method. (a) zinc-bound crystal structure of streptococcal pyrogenic exotoxin A (PDB ID: 1HA5), (b) Zn^{2+} -docked streptococcal pyrogenic exotoxin. Zn^{2+} represented in red bead.

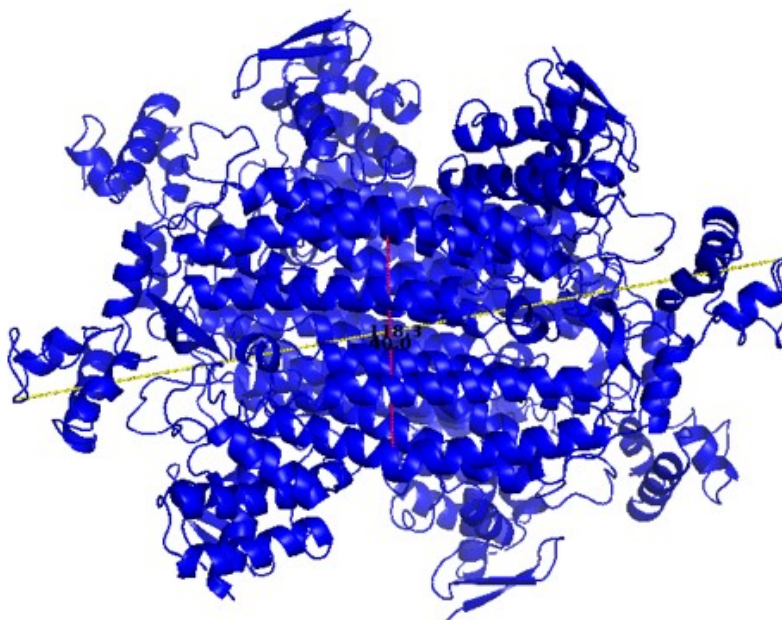


Figure S8. Crystal structure of *Saccharomyces cerevisiae* fumarase (PDB ID: 1YFM). The overall tetrameric enzyme is shown in cartoon representation. The approximate dimensions of the enzyme are $118.3 \times 40.0 \text{ \AA}$, measured along the longest and shortest molecular axes, respectively.

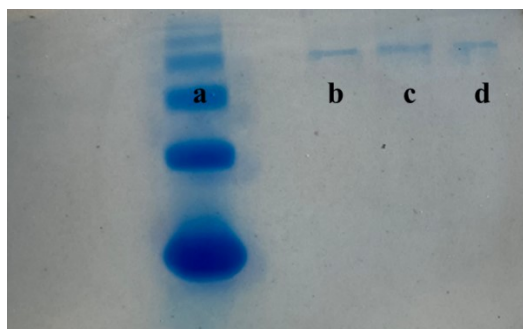


Figure S9. Native PAGE analysis of fumarase oligomerization. Lane (a) BSA as protein marker, (b) apo fumarase, (c) Zn^{2+} -treated fumarase, and (d) Zn(1)-CQD-treated fumarase. All samples show a single band with identical mobility, indicating that the tetrameric state of fumarase is maintained in the presence of Zn^{2+} and Zn(1)-CQDs.

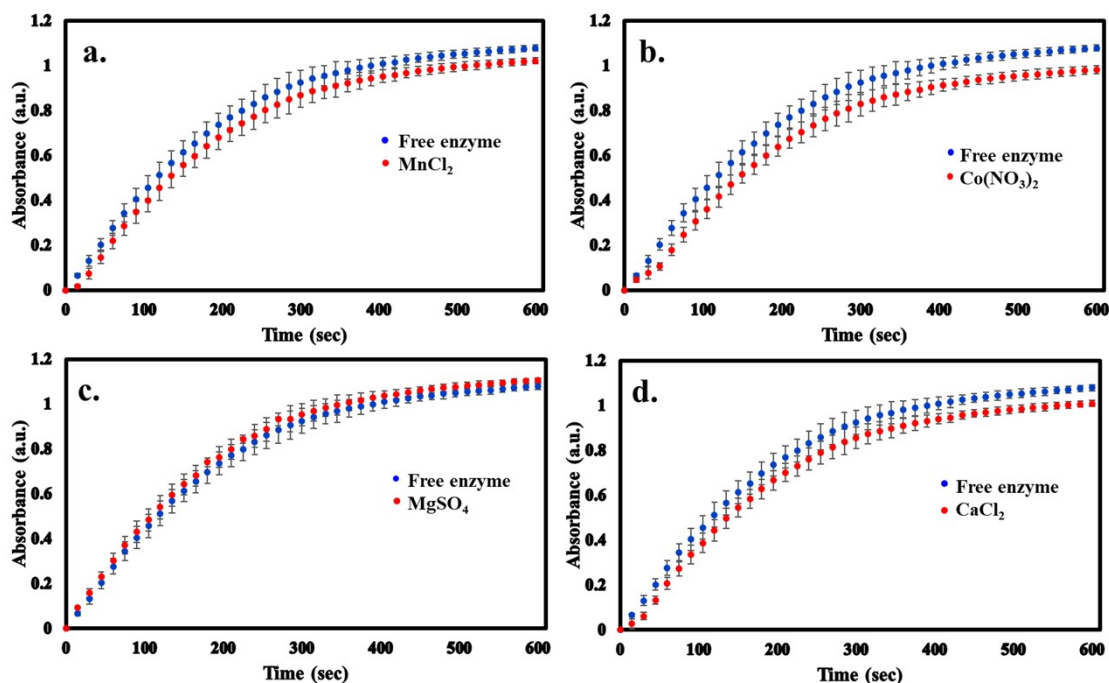


Figure S10. the effect of 200 μM (a) MnCl_2 , (b) $\text{Co}(\text{NO}_3)_2$, (c) MgSO_4 , and (d) CaCl_2 , on the fumarase activity in the conversion of fumarate to L-malate. The reaction contains 20 $\mu\text{g}/\text{mL}$ fumarase in 50 mM phosphate buffer pH 7. Each time point is an average of three independent experiments.

References

- (1) Stoscheck, C. M. [6] Quantitation of protein. In *Methods in enzymology*, Vol. 182; Elsevier, 1990; pp 50-68.
- (2) Hanwell, M. D.; Curtis, D. E.; Lonie, D. C.; Vandermeersch, T.; Zurek, E.; Hutchison, G. R. Avogadro: an advanced semantic chemical editor, visualization, and analysis platform. *Journal of cheminformatics* **2012**, *4*, 1-17.
- (3) Trott, O.; Olson, A. J. AutoDock Vina: improving the speed and accuracy of docking with a new scoring function, efficient optimization, and multithreading. *Journal of computational chemistry* **2010**, *31* (2), 455-461.
- (4) Baker, M.; Gutman, D. M.; Papageorgiou, A. C.; Collins, C. M.; Acharya, K. R. Structural features of a zinc binding site in the superantigen streptococcal pyrogenic exotoxin A (SpeA1): implications for MHC class II recognition. *Protein Science* **2001**, *10* (6), 1268-1273.
- (5) Abraham, M. J.; Murtola, T.; Schulz, R.; Páll, S.; Smith, J. C.; Hess, B.; Lindahl, E. GROMACS: High performance molecular simulations through multi-level parallelism from laptops to supercomputers. *SoftwareX* **2015**, *1*, 19-25.